



Proceedings of

International Conference on Science and Sustainable Development (ICSSD)

“The Role of Science in Novel Research and Advances in Technology”

Center for Research, Innovation and Discovery, Covenant University, Nigeria

June 20-22, 2017

Research Article

Application of Artificial Neural Network for the Inversion of Electrical Resistivity Data

O.L. Johnson and A.P. Aizebeokhai*

Department of Physics, Covenant University, Ota, Nigeria

*Corresponding author: a.p.aizebeokhai@gmail.com

Abstract. The inversion of most geophysical data sets is complex due to the inherent non-linearity of the inverse problem. This usually leads to non-uniqueness of solutions to the inverse problem. Artificial neural network (ANN) has been used effectively to address several non-linear and non-stationary inverse problems. This study is essentially an assessment of the effectiveness of estimating subsurface resistivity model parameters from apparent resistivity measurements using ANN. Multi-layered earth models for different geologic environments were used to generate synthetic apparent resistivity data. The synthetic apparent resistivity data were generated using linear filter method embedded in the RES1D program. Neural network toolbox on MATLAB was used to design, train and test a developed neural network that was employed in the inversion of the apparent resistivity sounding data sets. Resilient feed-forward back propagation algorithm was used to train the network. The network was trained with 50% of the synthetic apparent resistivity data sets and their corresponding multi-layered earth models. 25% of the data set was used to test the network and the network was validated with another 25% of the data set. The network was then used to invert field data obtained from Iyanna-Iyesi, southwestern Nigeria. The results obtained from ANN responses were compared with that of a conventional geoelectrical resistivity inversion program (WINRESIST); the results indicate that ANN is effective in the inversion of geoelectrical resistivity sounding data for multi-layered earth models.

Keywords. Artificial Neural Network (ANN)

MSC. 92B20

Received: May 23, 2017

Revised: June 19, 2017

Accepted: July 15, 2017

1. Introduction

The main goal of performing electrical resistivity survey is to evaluate the variations in the subsurface resistivity distribution based on the surface measurements of the apparent resistivity and interpret these variations (resistivity anomalies) in terms of geological and hydrogeological features in the subsurface. The true resistivity of the earth's subsurface can only be measured directly if the subsurface was to be homogeneous and this is never the case. Apparent resistivity, which is the volumetric average of the resistivity of a homogeneous half-space, depends on the electrode configuration used for the measurements (Aizebeokhai, 2010). This is because the subsurface layering and the geoelectric parameters of the layers are often unknown. The determination of the true resistivity model from the measured apparent resistivity data set is an inverse problem. Thus, the true resistivity distribution of the subsurface cannot be uniquely determined due to the intrinsic nature of the data structure. Also, the relationship between the observed apparent resistivity and the model parameters (true resistivity and layer thickness) is non-linear. Forward modelling mathematical techniques are generally used to relate the observed apparent resistivity to the desired model parameters. In other words, they are required to predict what the observed apparent resistivity should have been given the layered models.

Inversion techniques are commonly used to solve geophysical and engineering inverse problems (Tarantola, 2005). Inversion is performed on the measured apparent resistivity data to estimate the true model resistivity and thickness for each layer. Inversion is not only limited to resistivity data as nearly all geophysical problems are inverse problems. The normal linearized inversion methods to solving the non-linear inverse problem in geophysics are generally based on iterative processes. The inversion processes update the model parameters at each step to best fit the observed data. A good inversion method must simultaneously minimize the effects of the observed apparent resistivity data error and the model parameter errors. Conventionally, observed apparent resistivity field data and a starting model are inputted into the inversion program for inversion to produce calculated apparent resistivity with a final inverse model of the subsurface.

Advanced modern technology in computer forward modelling has made it possible to estimate resistivity data for 1D, 2D and 3D resistivity models of the subsurface. Advanced methods such as linear filter theory and exponential approximation of Kernel function are iterative methods which require quasi-linearization of the non-linear resistivity problem and adjust the model parameters iteratively to produce a response to some degree of agreement with the observed data. The least squares optimization method (Lines and Treitel, 1984) is commonly used for the data inversion. The initial model consisting of the different resistivity and thickness of the assumed layers is modified by the optimization process in order to increase the correlation between the measured and calculated apparent resistivity values. The least square inverse solutions are often unstable and not unique when applied to all non-linear inverse problems. The non-uniqueness may be due to a finite number of measurements of both current and potential sampling points.

The initialization of model parameters is important in normal inversion of resistivity data and poor hypothesis usually results in the wrong estimation of parameters. Artificial neural

network (ANN) may be used in the direct inversion of resistivity data as it has the ability to learn and perform non-linear optimization in the interpretation of geophysical data. ANN used in the direct inversion of resistivity data proceeds from observation and experience rather than theoretical deduction (Stephen et al., 2004). ANN can be used in the interpretation of 1D, 2D, 3D and 4D electrical resistivity data. Unlike the normal methods used for interpretation of resistivity data which use a fixed algorithm to estimate model parameters, ANN performs artificial intelligent non-linear interpretation between input and output data and allows the network to acquire useful information on the problem. A lot of data sets are used to train the network. ANN is a powerful data-driven, self-adaptive, flexible computational tool with the ability to perform nonlinear statistical modelling and provide a new substitute to logistic regression with a high degree of accuracy.

Neural networks offer a number of advantages, including imposing less formal statistical training, ability to implicitly detect complex nonlinear relationships between dependent and independent variables, ability to detect all possible interactions between predicting variables and the availability of multiple training algorithms. ANN with Back Propagation (BP) learning algorithm is widely used in solving various classical forecasting and estimation problems. The output performance will depend upon the trained parameters and the data set relevant to the training.

Inversion techniques commonly performed on resistivity data are used to deduce the distribution of the true resistivity of the subsurface. Interpreting resistivity data and obtaining an accurate model for the true resistivity of the subsurface is a problem as most solutions are unstable and not unique. Also, due to inhomogeneity and anisotropy, the interpretation may bring about ambiguous and unreliable results. ANN has the ability to be trained, can be used to analyse apparent resistivity data to produce more accurate models of the subsurface resistivity distribution; and thus, corrects for the ambiguity commonly observed in least-squares based inversions.

The aim of this study is to assess the effectiveness of estimating subsurface resistivity model parameters from resistivity measurements using artificial neural network (ANN). The specific objectives of this research are to estimate the electrical resistivity response of multi-layered earth model using ANN responses and compare the results obtained with those of conventional. The multi-layered earth models for different geologic environments were used to generate synthetic apparent resistivity data using the RES1D program for VES. The training of the neural network and testing of the data were carried out with the use of ANN tool box in MATLAB. The results obtained from the ANN were compared with that of the conventional inversion program, Win-Resist.

2. Theoretical Framework

Artificial Neural Networks (ANN) is a network of computer procedures (algorithms) inspired by the concept of the biological network of neurons which is used to approximately determine output functions that rely on a large amount of unknown inputs. It belongs to a group of computational designs inspired by the biological brains (Luger and Stubblefield, 1993; McClelland et al., 1986).

ANN is an artificial intelligence technology brought about by the analysis of the human central nervous systems. The human brain is made up of about 100 billion cells called neurons. These neurons are connected to each other through pathways called dendrites that help to receive electrical signals from other neurons and axons to transmit electrical signals to other neurons. These connections give neurons the ability to accept and send electrical signals which are responsible for the brain's function.

The neural network is a way to make computers create a model of the brain so as to perform some activities just as the brain can., for example, pattern recognition. Neural networks are characterized by a lack of explicit representation of knowledge; there are no symbols or values that directly correspond to classes of interest. Rather, knowledge is implicitly represented in the patterns of interactions between network components (Lugar and Stubblefield, 1993). In ANN, the synthetic nodes also called neurons or processing elements are to reproduce a biological neural network. ANN works like the human brain in the sense that the information is received by the network from the environment via a learning procedure and the strength of the connected neurons (weights) are then used to store the received information and also activated during the training or prediction.

Figure 1 shows three-layer architecture of a neural network design. The computer performs the operation layer by layer and also moving from left to right. For the inputs I_1 , I_2 and I_3 , corresponding outputs O_1 , O_2 and O_3 will be calculated for them. In the first layer, each neuron obtains its respective inputs directly from its input, and their output becomes $f(I_1)$, $f(I_2)$ and $f(I_3)$ as seen in Equation (1). The output O_1 , O_2 and O_3 then become the inputs to the hidden layers and the strength of connections $W_1, W_2, W_3, W_4, \dots, W_{12}$ are then used to calculate the output of the neurons in the hidden layer by multiplying their inputs O_1 , O_2 and O_3 by their corresponding strength of connection and adding them. The calculated output at the hidden layer then becomes the inputs to calculate the corresponding output at the next hidden layer. The same process for the calculation at the hidden layer is repeated at the output layer until the desired goal is achieved.

$$\begin{array}{ll}
 \text{Input Layer} & O_1 = f(I_1) \\
 & O_2 = f(I_2) \\
 & O_3 = f(I_3) \\
 \\
 \text{Hidden Layer} & O_4 = f((W_1 * O_1) + (W_5 * O_2) + (W_9 * O_3)) \\
 & O_5 = f((W_2 * O_1) + (W_6 * O_2) + (W_{10} * O_3)) \\
 & O_6 = f((W_3 * O_1) + (W_7 * O_2) + (W_{11} * O_3)) \\
 & O_7 = f((W_4 * O_1) + (W_8 * O_2) + (W_{12} * O_3)) \\
 \\
 \text{Output Layer} & O_8 = f((W_{13} * O_4) + (W_{16} * O_5) + (W_{19} * O_6) + (W_{22} * O_7)) \\
 & O_9 = f((W_{14} * O_4) + (W_{17} * O_5) + (W_{20} * O_6) + (W_{23} * O_7)) \\
 & O_{10} = f((W_{15} * O_4) + (W_{18} * O_5) + (W_{21} * O_6) + (W_{24} * O_7)) \quad (1)
 \end{array}$$

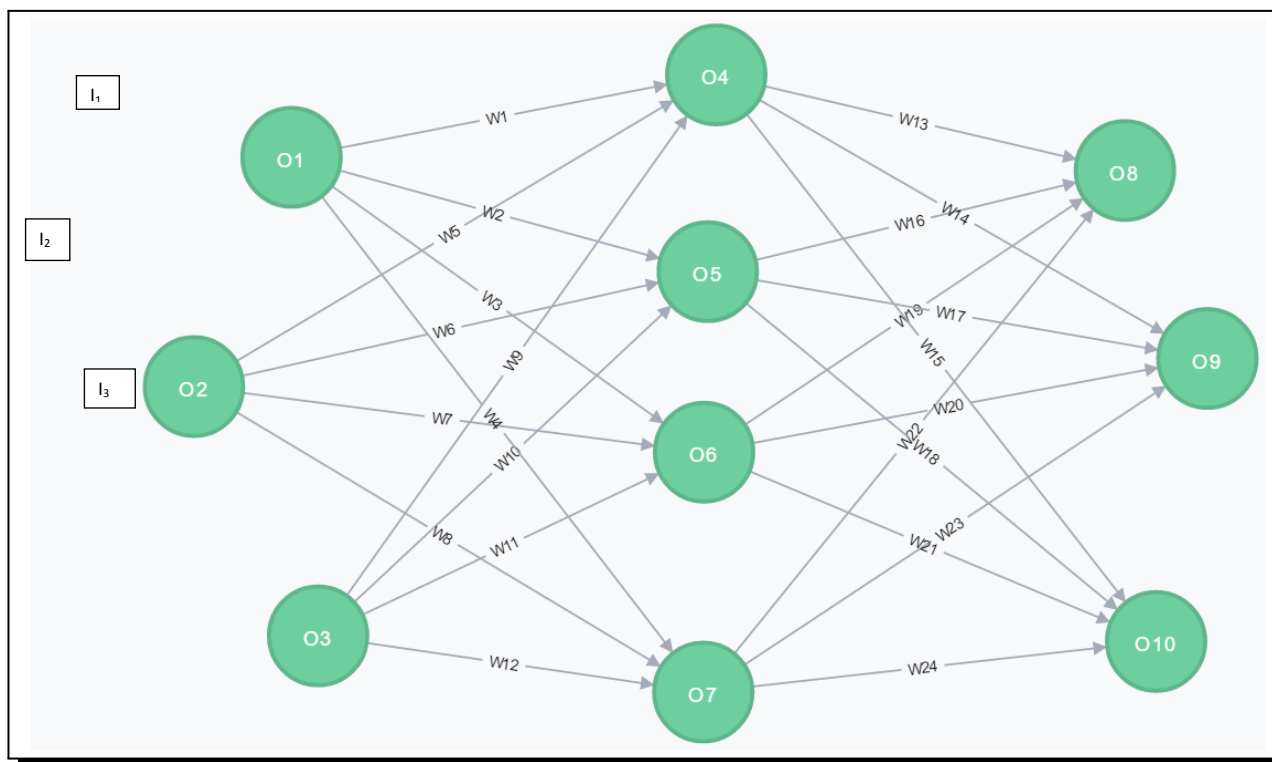


Figure 1. Three layer neural network architecture

3. Methodology

In this project, synthetic data sets were generated that mimic different geologic environments. Different models for 3-8 horizontal isotropic layers over a half-space were used to generate a set of apparent resistivities for 24 and 25 current electrode positions with half-current electrode spacing ($AB/2$) ranging from 1 m to 750 m and 1 m to 1000 m, respectively. These ranges of current electrode spacing were selected because the effective depth of investigation for these spread is similar to that of the test data (observed field data). The linear filter method (Koefoed, 1979) embedded in the RES1D program was used for the forward modelling to calculate the synthetic apparent resistivity for Schlumberger array on 1D earth models. The design, training and testing of the data were performed with the use of the Neural Network Toolbox on the MATLAB software (Demuth et al., 2007).

3.1 Synthetic Model Generation and Forward Modelling

The forward modelling for the 3-8 layered models were carried out with the use of the RES1D program. Tables 1 and 2 show the different earth layered models generated for 24 and 25 data points respectively. The following workflow was implemented for the synthetic model generation and forward modelling:

- (i) Generation of different models for different environments.
- (ii) Inputting the synthetic models into the RES1D program for forward modelling.

	3 LAYERS		4LAYERS		5 LAYERS		6LAYERS		7 LAYERS		8LAYERS		
	RESISTIVITY	THICKNESS											
24 DATA POINTS	MODEL 1	300	1.3	20	4.1	10	2	70	1.9	140	1.3	90.8	1.3
		50	10	60	3.6	50	11	340	7.4	540	3	320.7	4
		1200		22	12.5	100	20	405	20.8	1200	17	1101.5	10.7
	MODEL 2			1200		20	15	360	13.2	3800	20	3555.3	24
		1200	5			400		120	12.4	400	15	366.7	15.7
		50	12	60	3			700		120	14	110.6	11.4
	MODEL 3			10	10.8	84	1.4			100		90	9.5
		300		40	19.5	730	4	36	1.5			50	
				700		400	15	112	6.8	140	1.8		
	MODEL 4					280	20	332	15.5	330	4	70	1
						3000		4044	20.5	1800	11.7	720.7	2.5
								1860	14	3555.3	18	1201.5	6.7
	MODEL 5							799		366.7	13	1575.3	16.8
										110.6	11.4	3574.3	20.7
										54		370	14.2
	MODEL 6											90	9.5
												66.3	

Table 1. The different models generated for 24 data points

	3 LAYERS		4LAYERS		5 LAYERS		6LAYERS		7 LAYERS		8LAYERS		
	RESISTIVITY	THICKNESS											
25 DATA POINTS	MODEL 1	10	5	60	4	62.9	1.3	37	1.3	55	1.1	220.6	1.4
		390	10	100	11.5	1300	2.5	140	3.7	662	4.6	175.9	3.9
		10		40	20.3	3400	5.7	17	11.5	1020	15	1375	5
	MODEL 2			9000		380.5	15.4	340	15.7	2900	11	1790	15.8
		530	4.8			167		130	22.6	360	14	3990.8	21
		42	8	150	1			3065		120	13	360	19
	MODEL 3			30	4	222	1.3			60		220.5	14
		3		160	5	170.4	9.9	84.5	1.4			80	
				1000		1084	12.4	279.1	4.7	260	1.1		
	MODEL 4					1645	20.6	731.3	16.6	500	10	360	1.4
						4265		3084	18.3	90	17.3	1790	1.9
								484	12.8	1200	14	1375	5.9
	MODEL 5							170.9		100	15	80	15
										155	10.9	3990.8	21
										3080		220.5	14
	MODEL 6											175.9	

Table 2. The different models generated for 25 data points

After the generation of the different models, the model parameters were inputted into the RES1D program to calculate for their different apparent resistivities. Table 3 shows the generated apparent resistivities from the earth layered models.

AB/2	MODEL 1	MODEL 2	MODEL 3	MODEL 4	MODEL 5	MODEL 6	MODEL 7	MODEL 8	MODEL 9	MODEL 10	MODEL 11	MODEL 12
1	281.9074	1198.047	20.0326	59.6496	10.2122	89.8217	71.6938	37.2815	148.6465	142.4666	96.084	82.3408
1.3	284.6472	1201.218	19.9899	60.0313	10.1287	90.6532	71.1589	37.2634	150.1526	141.6176	96.9593	88.3168
1.8	236.3762	1191.295	20.1479	58.4751	10.913	106.9314	77.2089	41.1125	172.989	150.3737	110.9275	112.5651
2.4	183.152	1174.058	20.4259	55.922	12.1459	130.1422	86.5774	46.5748	204.4208	163.7294	130.0636	144.3645
3.2	135.0785	1144.08	20.9007	51.9693	13.8731	158.5149	99.4124	53.2701	241.8338	181.9347	152.7472	181.2916
4.2	95.9512	1086.294	21.7638	45.7339	16.3103	193.1402	117.0353	61.4766	287.3561	207.4464	180.3586	225.4241
4.2	72.3133	983.4559	23.1983	37.2975	19.4212	232.9653	138.9732	70.9978	341.8334	241.3523	213.7879	278.6859
5.5	61.6324	793.2405	25.5834	26.7863	23.6388	281.4209	167.8981	83.4475	415.9658	293.002	261.093	351.9995
7.5	62.4501	562.1244	28.2221	19.1738	28.0371	325.4566	197.0721	97.2904	497.9474	357.4312	317.3253	433.451
10	69.2182	352.9813	30.5521	15.5267	32.3947	360.688	224.5983	113.1052	583.9692	433.5599	381.933	519.527
13	85.857	172.069	33.2405	14.947	38.2749	393.1063	258.5656	139.3008	704.7746	552.548	482.7328	642.1257
13	109.0758	110.1274	36.3009	17.0807	43.9239	410.1079	286.8188	170.9266	823.5078	678.2778	592.3186	764.0883
18	140.6697	103.3922	41.6112	20.95	49.8511	420.2147	311.381	213.0672	951.0724	816.3682	719.405	895.4045
24	178.5687	118.5338	50.3339	26.1645	55.3723	432.5603	329.3491	265.1029	1072.505	945.0693	848.119	1020.947
32	224.6862	140.45	63.3688	33.1481	60.4935	461.5103	341.2754	330.2325	1173.382	1047.094	966.6311	1131.482
42	289.3534	166.4711	84.3511	43.9976	66.539	532.1308	350.4432	421.7843	1220.38	1090.29	1054.722	1204.867
55	361.0891	191.4717	110.0134	57.3753	74.1069	643.7273	361.7733	519.2083	1150.738	1019.608	1047.415	1175.001
55	436.1804	213.3471	139.5482	72.8986	84.8775	781.726	382.4956	612.8796	977.6263	852.8359	941.4194	1038.395
75	540.414	237.7696	185.8738	97.4243	104.9457	992.866	425.295	723.8035	666.9729	561.0386	691.5442	745.9925
100	639.6306	255.8833	237.2056	124.8154	128.7191	1209.105	473.9864	804.075	396.0087	310.4438	429.6196	454.1031
130	740.9658	270.1633	299.3944	158.3033	156.8213	1446.896	524.1378	856.9236	217.0524	149.8797	219.1758	232.8977
130	833.9142	280.2102	368.6165	195.9778	186.2987	1683.434	567.5466	878.1603	138.3216	82.143	107.1135	121.317
180	918.8185	287.2793	446.9565	239.1429	217.2926	1919.24	604.2441	876.1055	110.9685	60.7254	65.9164	81.3736
240	1002.778	292.6168	547.2454	295.2764	253.4572	2177.398	637.4046	858.0604	104.1838	56.2407	53.1574	69.9218

Table 3. Apparent resistivities generated from the different models

3.2 Design, Training and Testing of Network

The NN toolbox software delivers a flexible network object type that permits different architectures of networks to be generated and then used with different functions to initialize, train and simulate. This flexibility is obtained because the generated networks have an object-oriented representation. The representation permits the design of different architectures and also allocates various algorithms to the architectures. In this work, a multilayer feed forward network was implemented from the neural network tool box. This can be used for function fitting, pattern recognition problems and prediction problems. The following work flow was implemented using the neural network tool box for training network:

- (i) Arrangement of apparent resistivity and layered model data.
- (ii) Create and configure the network.
- (iii) Train the network.
- (iv) Validate and test the network.
- (v) Use the network on the field data.

3.3 Data Arrangement

The effectiveness of any network depends mainly on the arrangement of the data used in the training and testing of the network. The effectiveness of any network depends mainly on the arrangement of the data used in the training and testing of the network. The data used consisted of the generated synthetic earth layered models, their corresponding apparent resistivities and the apparent resistivities from the field data. The generated synthetic earth layered models and their corresponding apparent resistivities were divided into two sets for the training, i.e. twenty four (24) data points and twenty five (25) data points. Twenty four data points consists of twenty four datasets of four (4) of each earth layered models in .MOD format and their corresponding apparent resistivities in .DAT format while the twenty five data points consists of twenty four datasets of four (4) sets of each layered earth models in .MOD and their corresponding apparent resistivities in .DAT format. The network was also trained with some sets of the apparent resistivities from the field data. The testing data consists of sets of twenty four and twenty five data points of the generated apparent resistivities and also the apparent resistivities from the field.

Tables ?? and ?? show the arrangement of the input and target data sets into the MATLAB program for training the network respectively. The network's input and target matrices were a $24 \times N$ and $M \times N$ matrix respectively for 24 data points and $25 \times N$ and $M \times N$ matrix for 25 data points, where N is the number of soundings, M is the earth layered models consisting of the true resistivity and thicknesses. Most times, the data has to be transposed to be inputted into the neural network architecture for training. So therefore, the input and target matrices

are a $N \times 24$ and $N \times 25$ for 24 and 25 data points respectively, where N here is the number of inputs and 24 and 25 are the number of samples.

3.4 Neural Network Architecture Design

Designing a neural network on MATLAB can be done by using the conventional neural network toolbox or coding the architecture. Figure ?? shows the conventional way of designing a network and this is prompted using the 'nntool' command. This involves giving the network a name, setting the input data, the target data, the training function, adaption learning function, the adaptation learning function, performance function, etc.

The following are the requirements to design a neural network:

- (i) Configuration of the inputs, layers and outputs.
- (ii) Normalization of the input data.
- (iii) Setting the transfer function for each layers.
- (iv) Setting the Initialization, Performance, Training and Divide Functions.
- (v) Setting the training parameters.
- (vi) Viewing the network.

4. Application of Neural Network to Field Data

ANN was applied to estimate the earth layered models for a field in Ota, Ogun State. After the network is trained, tested and validated, the network will then be used to calculate its response to any input. The field apparent resistivity data was used as an input to estimate its earth layered model which consists of the true resistivities and the thicknesses. The 'sim' function is used to simulate the neural network to estimate the earth model parameters. 'sim(project, TEST_FIELD1_8LAY)' is used to estimate the model parameters for the input field apparent resistivity contained in the matrix 'TEST_FIELD1_8LAY' and for the neural network 'project'. The 'mse' function was used to calculate the mean square error between targets and output. 'mse(project, FIELD_TARGET, project_output)' was used to calculate the mean square error between the target data contained in the matrix 'FIELD_TARGET' and the network's output 'project_output'.

5. Results and Discussions

After series of iterations, the network showed its effectiveness in estimating the earth layered models. A good fit between the target and output data was achieved on a trial and error basis. After the arrangement and normalization of the input and target data, the number of inputs used for the architecture was 24 and 25 for twenty four (24) and twenty five (25) data points respectively. The transfer function for the hidden layers used was the log sigmodial transfer

function. The target data was arranged at different time steps containing ‘NaN’ values for areas with no data. The ‘divideblock’ function was used to divide the input and target matrices for training, testing and validation, where 50% was used for training, 25% for testing and 25% for validation. This division was done because of the arrangement of the data. In most cases, it is advisable to use 70% for training, 15% for testing and the other 15% for validation. So of the 24 sample data sets used, 12 were used for training, 6 for testing and the remaining 6 used for validation. After series of iterations, the network adapted to the data, was tested with the generated synthetic models and was used to estimate the earth layered models for the field data. After the first few iterations, the regression values obtained were not good enough. The number of neurons was increased from 20 to 30 and so on and this improved the results of the iteration. After a lot of iterations, the data adapted almost perfectly to the network but after the number of hidden neurons was increased, the network began to adapt faster to the network and a better fit between the target and output data was obtained.

Figures 2a and 2b are the neural network architectures used for the input and target matrices for 25 and 25 data points respectively. Figure 3a is one the best fits between the target and output data, Figure 3b is the performance plot and Figure 3c is the training state of the network. Tables 4 to 9 show the different synthetic earth layered models and the estimated earth layered models from WINRESIST and ANN.

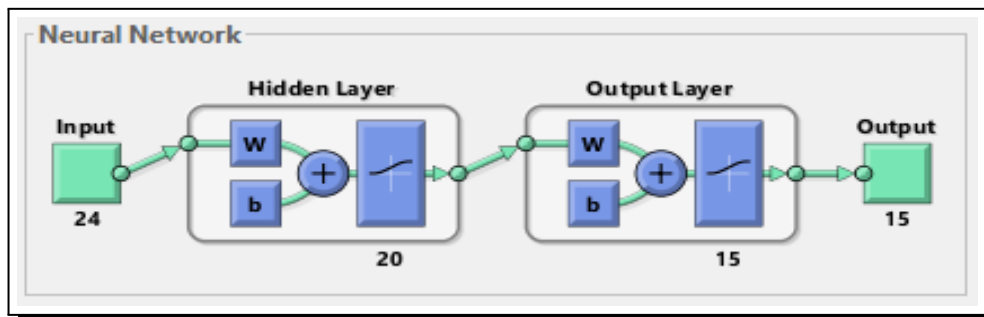


Figure 2a. Neural network architecture for 24 data points

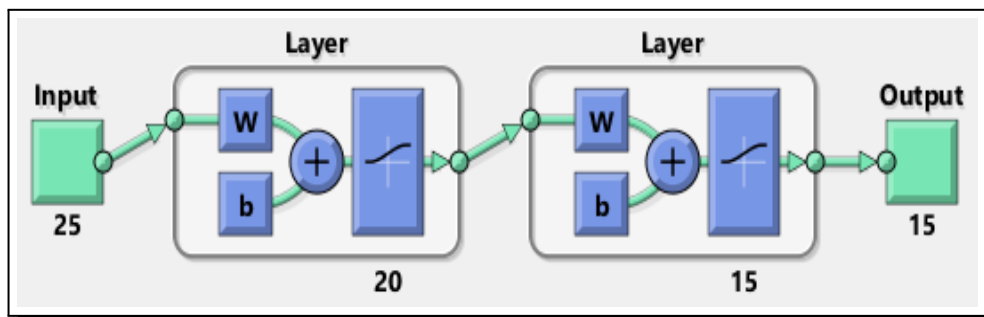


Figure 2b. Neural network architecture for 25 data points

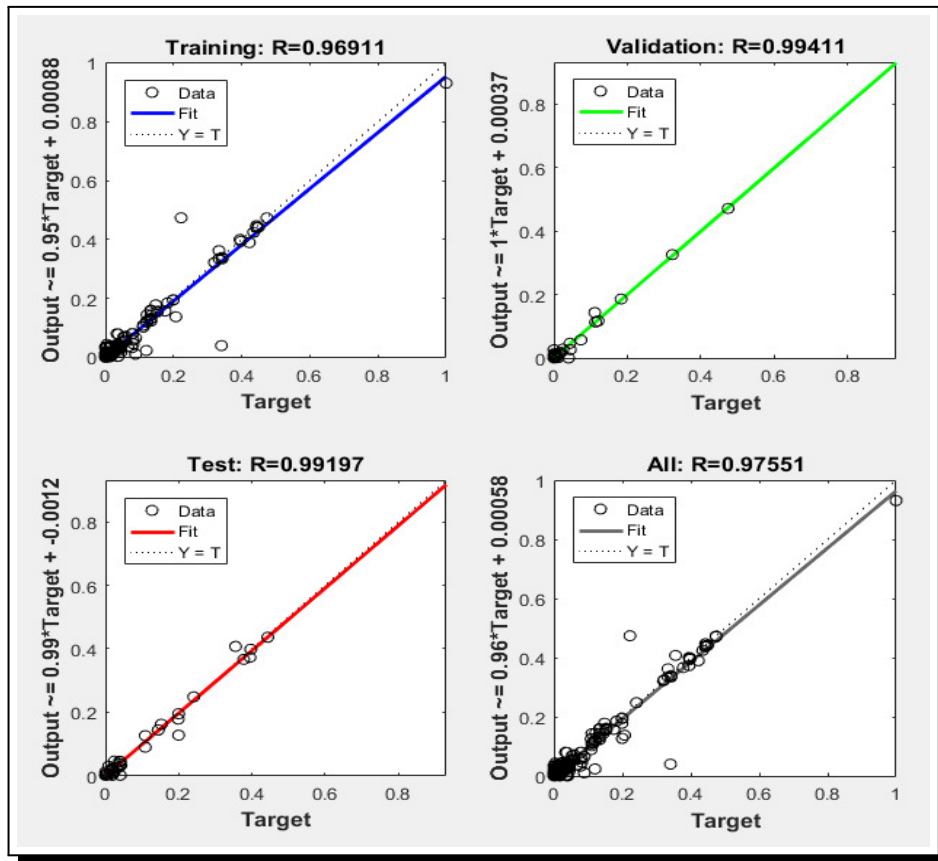


Figure 3a. One of the best regressions fit after series of iterations

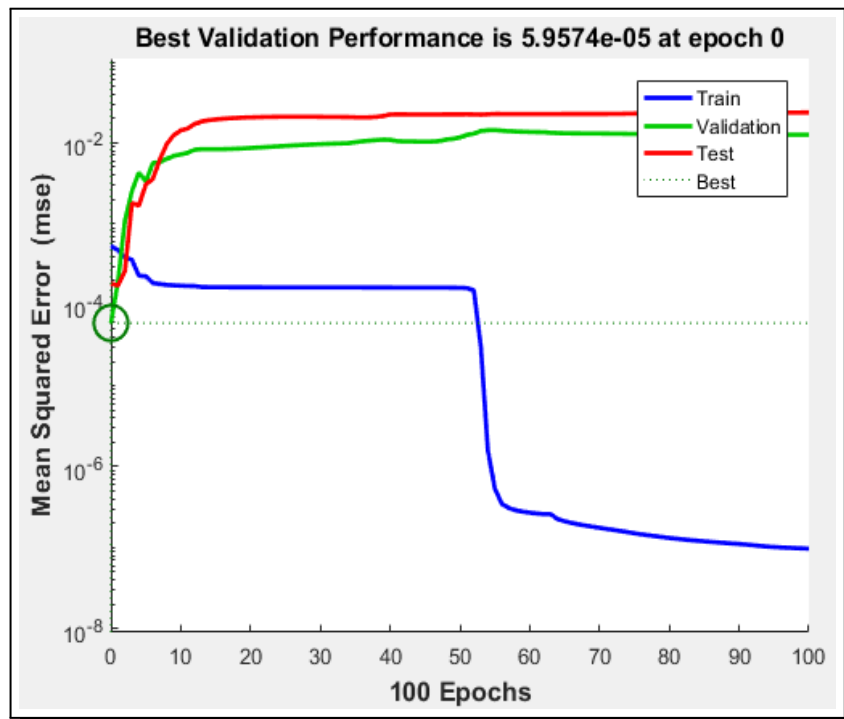


Figure 3b. Performance plot of the network after series of iterations

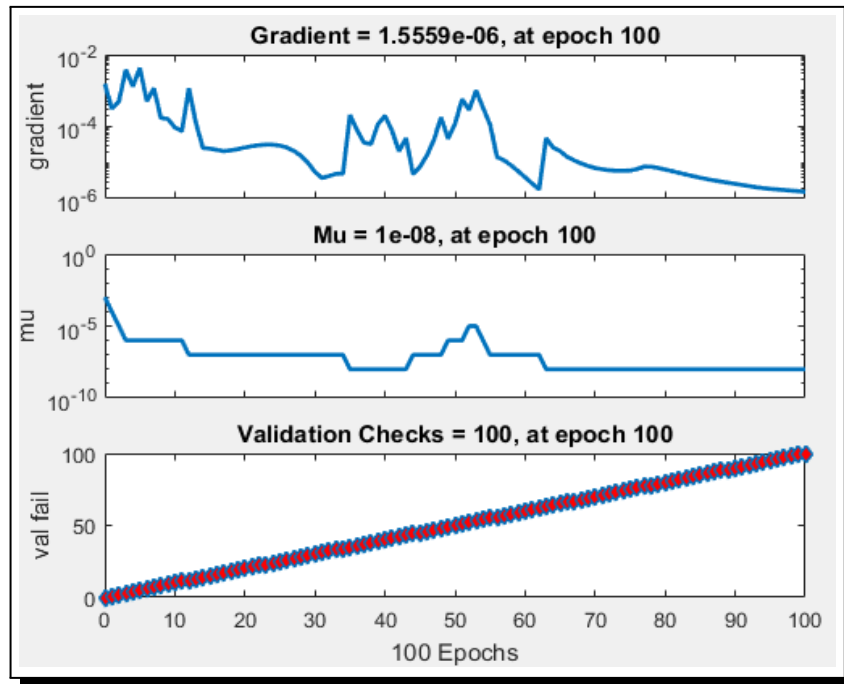


Figure 3c. Training state of the network after series of iterations

		3 LAYER MODELS												
		RES 1D MODELS		WINREST MODELS			ANN MODELS							
		RES	THICKNESS	RES	THICKNESS	RMS ERROR	RES	THICKNESS	MSE ERROR	RMS ERROR				
24 DATA POINTS	MODEL 1	300.0	1.3	311.3	1.3	0.5	USED FOR TRAINING							
		50.0	6.0	51.0	5.8	0.0								
		28.0	0.0	28.0	0.0	0.0								
		8.0	5.0	8.0	5.1	0.5								
		20.0	8.0	20.4	7.8	0.0								
		5.0	0.0	5.0	0.0	0.0								
	MODEL 2	1900.0	4.9	1902.9	4.9	2.1					1899.615297	5.607115	0.0	0.0
		50.0	9.0	48.3	9.3	0.0					50.546735	10.044550	0.0	0.0
		29.5	0.0	29.5	0.0	0.0					29.475623	NaN	0.0	0.0
		224.5	5.0	224.9	4.8	0.5					224.499578	5.956748	0.0	0.0
		99.0	12.0	102.7	11.4	0.0					99.028205	12.039630	0.0	0.0
		55.5	0.0	55.6	0.0	0.0					55.522386	NaN	0.0	0.0

Table 4. Three layered earth models from RES 1D and estimated models from WINRESIST and ANN

		4 LAYER MODELS										
		RES 1D MODELS		WINREST MODELS			ANN MODELS					
		RES	THICKNESS	RES	THICKNESS	RMS ERROR	RES	THICKNESS	MSE ERROR			
24 DATA POINTS	MODEL 9	200.0	4.1	200.2	4.2	0.1	USED FOR TRAINING					
		600.0	3.6	604.1	3.5							
		400.0	12.5	406.0	12.6							
		1000.0	0.0	998.8								
		420.0	5.0	419.5	5.4	0.1						
		380.0	11.3	377.2	11.0							
	MODEL 10	285.0	18.0	289.8	18.5							
		1002.0	0.0	1005.6								
		90.0	3.6	89.6	3.6	0.1				90.206397	3.607892	
		1508.0	12.0	1516.1	12.0					1510.025691	12.124567	
		1000.0	3.6	1000.2	3.4					1002.679834	3.629856	
		300.0	0.0	300.1						303.458933	NaN	
MODEL 11	60.0	3.0	59.6	3.0	0.1	61.985678	3.005789					
	500.0	10.8	506.4	10.6		499.236791	10.798765					
	400.0	3.0	402.7	3.0		399.219809	3.287865					
	60.0	0.0	60.1			61.789076	NaN					
MODEL 12												

Table 5. Four layered earth models from RES 1D and estimated models from WINRESIST and ANN

		5 LAYER MODELS							
		RES 1D MODELS		WINREST MODELS			ANN MODELS		
		RES	THICKNESS	RES	THICKNESS	RMS ERROR	RES	THICKNESS	MSE ERROR
MODEL 17		10.0	2.0	9.9	2.0	0.2	USED FOR TRAINING		
		50.0	11.0	51.2	10.5				
		100.0	20.0	90.0	24.5				
		200.0	2.0	237.3	1.9				
		50.0	0.0	49.7					
MODEL 18		500.0	1.0	498.6	1.0	0.4			
		1011.3	2.5	1040.3	2.4				
		600.0	13.5	594.1	12.7				
		400.0	1.0	405.9	1.4				
		1900.0	0.0	1898.4					
MODEL 19		90.0	1.3	86.9	1.2	0.3	92.989800	1.300456	
		320.0	3.0	299.6	3.0		322.467810	3.892561	
		1000.0	12.4	1005.9	12.4		1002.569810	12.450981	
		320.0	1.3	319.5	1.3		321.903801	1.325698	
		1008.0	0.0	1007.4			1010.589352	NaN	
MODEL 20		84.0	1.4	81.4	1.4	0.4	82.567892	1.402561	
		730.0	4.0	733.3	4.0		729.985701	5.290851	
		400.0	15.0	398.4	15.0		401.751502	15.085612	
		908.0	1.4	909.9	1.2		910.908376	1.435619	
		2090.0	0.0	2089.6			2100.108273	NaN	

Table 6. Five layered earth models from RES 1D and estimated models from WINRESIST and ANN

		6 LAYER MODELS							
		RES 1D MODELS		WINREST MODELS			ANN MODELS		
		RES	THICKNESS	RES	THICKNESS	RMS ERROR	RES	THICKNESS	MSE ERROR
MODEL 25		70.0	1.9	68.8	1.9	0.2	USED FOR TRAINING		
		1000.0	7.4	1192.5	6.2				
		405.0	20.8	376.8	20.6				
		360.0	13.2	373.6	12.1				
		1200.0	12.4	1229.6	12.6				
MODEL 26		700.0	0.0	696.8					
		145.0	1.0	142.7	1.0	0.2			
		900.0	2.5	959.7	2.4				
		298.5	8.3	286.7	8.2				
		447.0	2.5	456.9	2.5				
MODEL 27		50.0	2.5	51.8	2.5				
		150.0	0.0	149.9					
		55.0	1.4	53.5	1.4	0.3	52.097254	1.872538	
		306.0	7.9	304.3	7.8		302.678152	8.746291	
		1080.0	11.4	1074.4	11.5		1082.087361	11.481654	
MODEL 28		596.0	25.5	594.6	25.3		599.092735	26.019275	
		339.0	15.7	341.1	16.0		340.916274	15.610293	
		210.0	0.0	209.9			211.082675	NaN	
		36.0	1.5	35.3	1.5	0.1	35.890182	34.093856	
		112.0	6.8	112.8	6.9		113.028372	6.726154	
		3078.0	15.5	3064.3	15.9		3080.937186	16.019854	
		4044.0	20.5	3998.2	20.8		4045.728945	20.456172	
		1860.0	14.0	1852.7	14.0		1865.836178	14.293816	
		799.0	0.0	796.9			801.289375	NaN	

Table 7. Six layered earth models from RES 1D and estimated models from WINRESIST and ANN

		7 LAYER MODELS							
		RES 1D MODELS		WINREST MODELS			ANN MODELS		
		RES	THICKNESS	RES	THICKNESS	RMS ERROR	RES	THICKNESS	MSE ERROR
MODEL 33		140.0	1.3	136.5	1.3	0.3	USED FOR TRAINING		
		540.0	3.0	552.2	3.1				
		1200.0	17.0	1202.5	17.0				
		540.0	20.0	546.5	20.7				
		2000.0	15.0	1976.8	14.9				
MODEL 34		120.0	14.0	119.9	14.0				
		100.0	0.0	100.2					
		160.0	1.7	157.3	1.7	0.3			
		550.0	5.0	549.3	5.0				
		1500.0	11.7	1494.5	16.0				
MODEL 35		2006.7	19.3	2009.2	19.3				
		1650.9	15.5	1649.9	15.5				
		120.0	11.4	121.0	15.0				
		80.0	0.0	80.1					
		24.0	1.0	23.0	1.0	0.4	22.781625	1.103870	
MODEL 36		980.0	3.0	1025.0	3.0		989.982736	3.189172	
		1750.0	8.0	1789.7	8.0		1740.027351	8.261767	
		1800.0	11.0	1810.4	10.9		1827.082647	11.937648	
		3200.0	18.0	3179.0	17.9		3202.829101	18.937264	
		350.0	12.0	349.7	12.0		351.298364	12.391826	
MODEL 36		200.0	0.0	201.0			201.572810	NaN	
		140.0	1.8	154.8	1.6	0.5	133.999453	2.587201	
		990.0	4.0	532.2	5.1		989.995156	3.897030	
		2807.0	11.7	1517.6	16.8		2806.990882	11.690239	
		3555.3	18.0	3799.2	16.9		3554.221287	18.011702	
		2900.0	13.0	379.6	15.7		2900.012984	12.935829	
		110.6	11.4	120.5	14.0		110.601232	11.380670	
	54.0	0.0	81.7			54.002243	NaN		

Table 8. Seven layered earth models from RES 1D and estimated models from WINRESIST and ANN

		8 LAYER MODELS						
		RES 1D MODELS		WINRESIST MODELS			ANN MODELS	
		RES	THICKNESS	RES	THICKNESS	RMS ERROR	RES	THICKNESS MSE
MODEL 41		30.8	1.3	88.7	1.3	0.3		
		320.7	4.0	324.4	4.0			
		900.0	10.7	899.0	10.8			
		1362.0	24.0	1355.0	24.3			
		356.7	15.7	356.5	15.1			
MODEL 42		110.6	11.4	110.1	11.0			
		90.0	9.5	90.1	9.0			
		50.0	0.0	50.0				
		187.9	1.4	186.3	1.4	0.4		
		280.8	3.9	282.5	3.9			
MODEL 43		1208.0	7.5	1223.1	7.9			
		2170.3	14.8	2217.0	14.7			
		3574.3	20.0	3556.3	19.8			
		370.0	19.0	369.4	19.0			
		960.0	14.0	975.9	13.9			
MODEL 44		80.9	0.0	81.4				
		187.9	1.0	183.4	1.0	0.2	187.900275	1.000000
		900.0	2.5	947.2	2.9		899.993120	2.500000
		1344.0	6.7	1411.9	6.9		1343.989145	6.700000
		2170.3	14.8	2178.5	14.6		2169.887950	14.800000
MODEL 45		1588.0	20.7	1564.0	20.4		1588.010652	20.700000
		50.0	15.6	49.9	16.0		50.001959	15.600000
		120.9	14.1	120.1	13.9		120.903070	14.100000
		50.1	0.0	50.0			50.087080	NaN
		70.0	1.0	67.6	1.0	0.1	68.990608	1.639724
MODEL 46		720.7	2.5	771.7	2.9		700.355661	2.057161
		1201.5	6.7	1261.4	6.9		1416.479116	6.427065
		1575.3	16.8	1550.6	16.8		1575.082019	16.961700
		720.7	20.7	710.3	20.4		706.295714	18.596160
		370.0	14.2	367.2	13.8		367.544429	12.447457
MODEL 47		90.0	9.5	89.5	10.0		76.481085	7.072557
		66.3	0.0	66.2			60.097707	NaN

Table 9. Eight layered earth models from RES 1D and estimated models from WINRESIST and ANN

5.1 Results of the Field Data

After successfully training the network and it has the ability to correctly estimate a model that was not used for training, the ANN will definitely be able to estimate the earth layered models for the apparent resistivities got from the field. Table 10 shows the responses of the trained ANN for the inputted apparent field resistivity data compared to that obtained from WINRESIST. Figures 10 and 11 are the sounding curves obtained after interpreting the field data using WINRESIST program while Figures 12 and 13 are their corresponding sounding curves obtained for the ANN responses.

6. Conclusion

The results obtained from ANN responses for the synthetic apparent resistivity data sets were compared with the corresponding earth layered models and also with that of WINRESIST. The compared results were almost the same as ANN was effective in estimating the models back in some cases. Figure 4 to Figure 9 shows the deviations in the compared results.

The arrangement of the input and target data sets used for the training of the network was a combination of different multiple earth layered models. This arrangement helped to mimic different environments and this makes the network very versatile in its learning and in the estimation of the model parameters. Figure 14 shows the contributed architecture of the neural network implemented in this research project. The architecture consists of 24 inputs labelled $R_{a1}, R_{a2}, \dots, R_{a24}$ which are the apparent resistivities, the hidden processing elements (neurons) which are labelled $PE1, PE2, \dots, PE_n$ and the targets, the corresponding multi-layered earth models which are labelled $Rt1 \dots Rt3$ and T_o for a three layered earth model and $Rt1_1 \dots Rt8_1$ and T_o_1 for an eight layered earth model.

	WINRESIST			ANN	
	RESISTIVITY	THICKNESS	RMS	RESISTIVITY	THICKNESS
VES 3	128.3	1.2	4.9	125.813527	1.973836
	225.0	2.7		342.628196	3.581927
	2408.2	4.1		2669.491624	2.907498
	9389.9	23.4		8899.671526	19.983625
	379.5	12.9		276.657182	13.826152
	119.4	13.0		373.271836	15.361728
	48.5			77.962186	NaN
VES 7	203.3	1.0	4.5	213.561926	1.116253
	54.7	1.9		55.816273	2.192837
	678.6	2.8		676.271625	3.137829
	2655.3	6.7		2654.172819	6.192837
	5117.9	21.7		5122.261738	21.819273
	364.6	12.2		367.261728	12.471829
	120.9	12.0		130.291829	12.192372
43.7			42.182937	NaN	
VES 8	84.5	1.4	2.8	51.517264	0.841725
	279.1	4.7		344.427183	4.917280
	731.3	16.6		662.918274	22.618274
	3084.0	30.3		2857.718274	31.618264
	484.0	12.8		482.417264	12.318274
	170.9			200.611716	NaN
VES 13	63.0	1.0	2.5	56.027384	1.391728
	338.0	1.9		379.810298	1.491835
	831.9	25.8		846.019284	26.192819
	3354.3	27.9		706.710294	28.192837
	403.3	14.1		3560.920192	14.192817
	120.3	13.0		396.210190	13.182729
	70.4			122.129200	NaN
VES 18	94.5	1.8	3.6	93.100294	1.723300
	828.9	4.0		295.102930	4.221000
	1840.9	11.4		2073.812018	10.210009
	3509.9	21.4		3739.201823	20.311910
	363.7	14.7		362.710297	14.310234
	118.6	13.9		117.510291	13.801820
	52.0			43.519210	NaN
VES 25	159.8	1.7	1.5	145.311029	1.600000
	558.2	5.5		609.534173	5.813011
	1488.9	16.4		1473.600385	15.401029
	3571.4	28.1		3751.111204	27.703873
	373.2	15.5		372.710294	15.519203
	121.5	14.1		121.410294	14.129104
	57.2			51.901829	NaN
VES 26	53.5	1.2	2.7	51.619274	1.100000
	166.0	2.5		160.700000	2.893040
	966.3	6.0		1082.371826	5.638394
	1953.1	14.1		2093.281729	13.903895
	3490.5	25.2		3474.300000	24.804293
	369.4	15.3		369.251395	15.209838
	120.7	14.0		120.428385	14.020193
	54.6			52.919204	NaN

Table 10. ANN response to inputted apparent resistivity from the field with WINRESIST

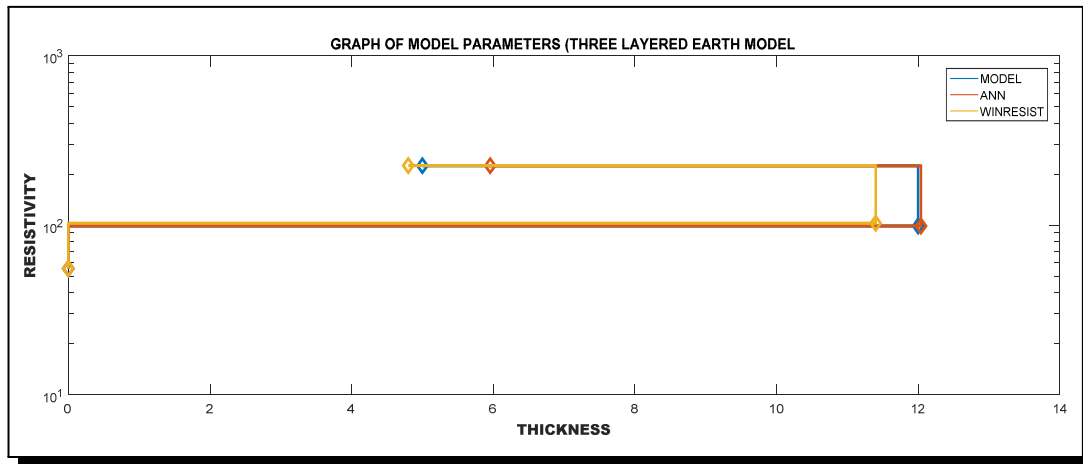


Figure 4. ANN responses compared with synthetic model parameters for three layered earth model

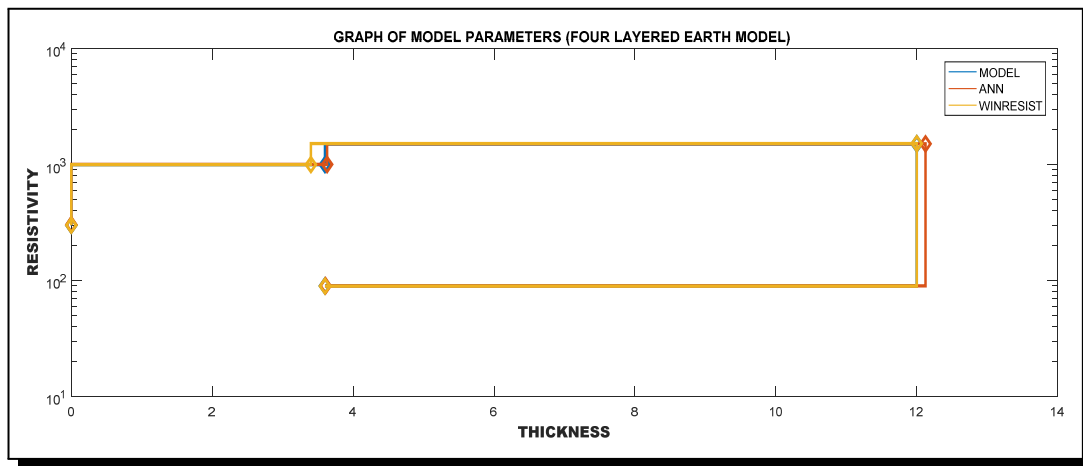


Figure 5. ANN responses compared with synthetic model parameters for four layered earth model

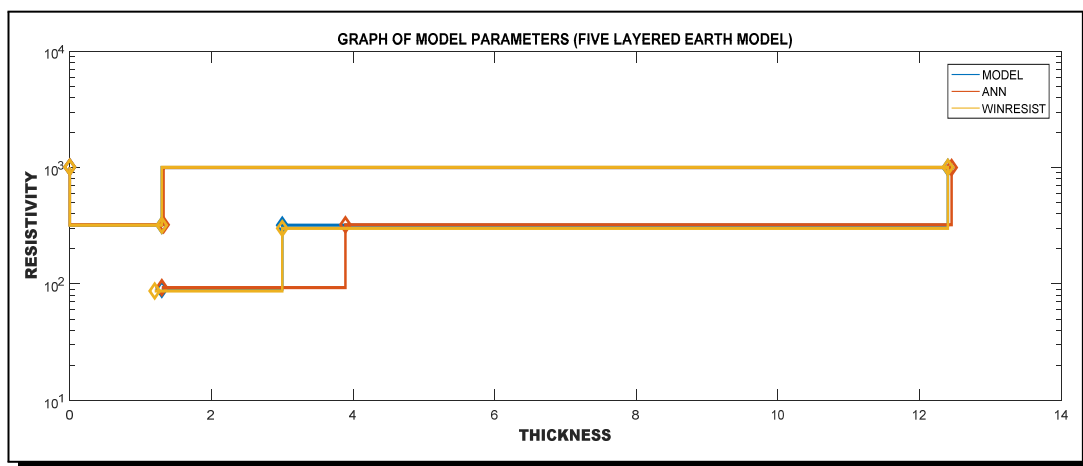


Figure 6. ANN responses compared with synthetic model parameters for five layered earth model

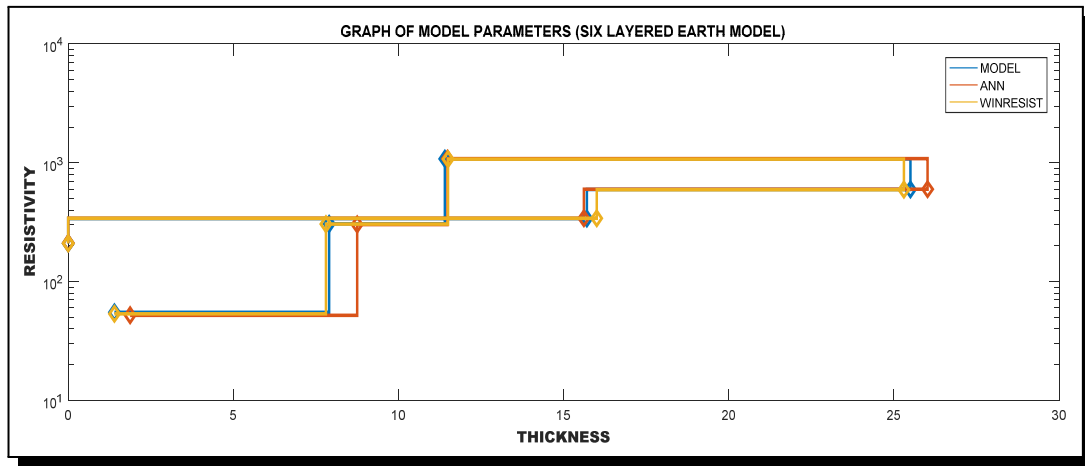


Figure 7. ANN responses compared with synthetic model parameters for six layered earth model

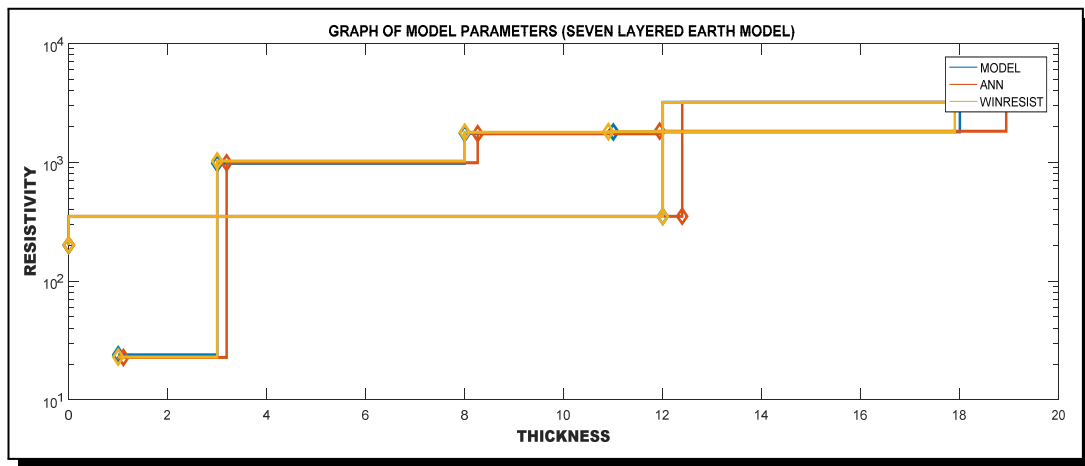


Figure 8. ANN responses compared with synthetic model parameters for seven layered earth model

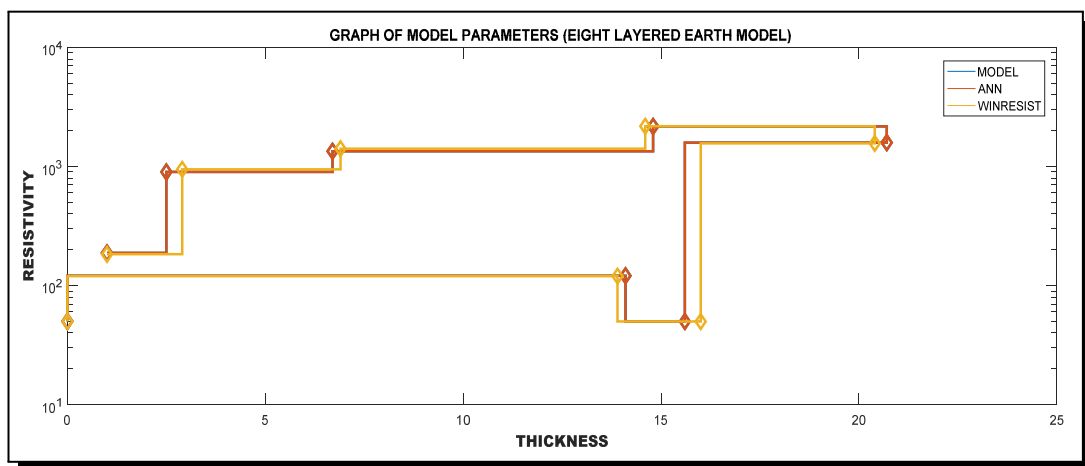


Figure 9. ANN responses compared with synthetic model parameter for eight layered earth model

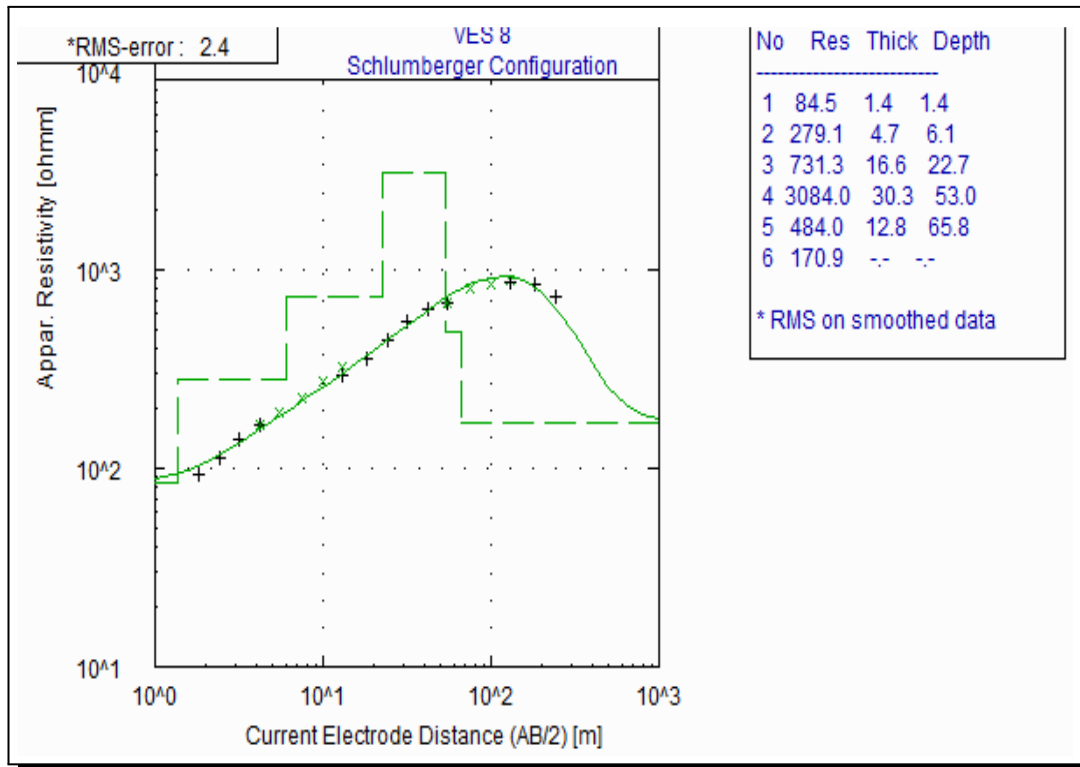


Figure 10. VES 8

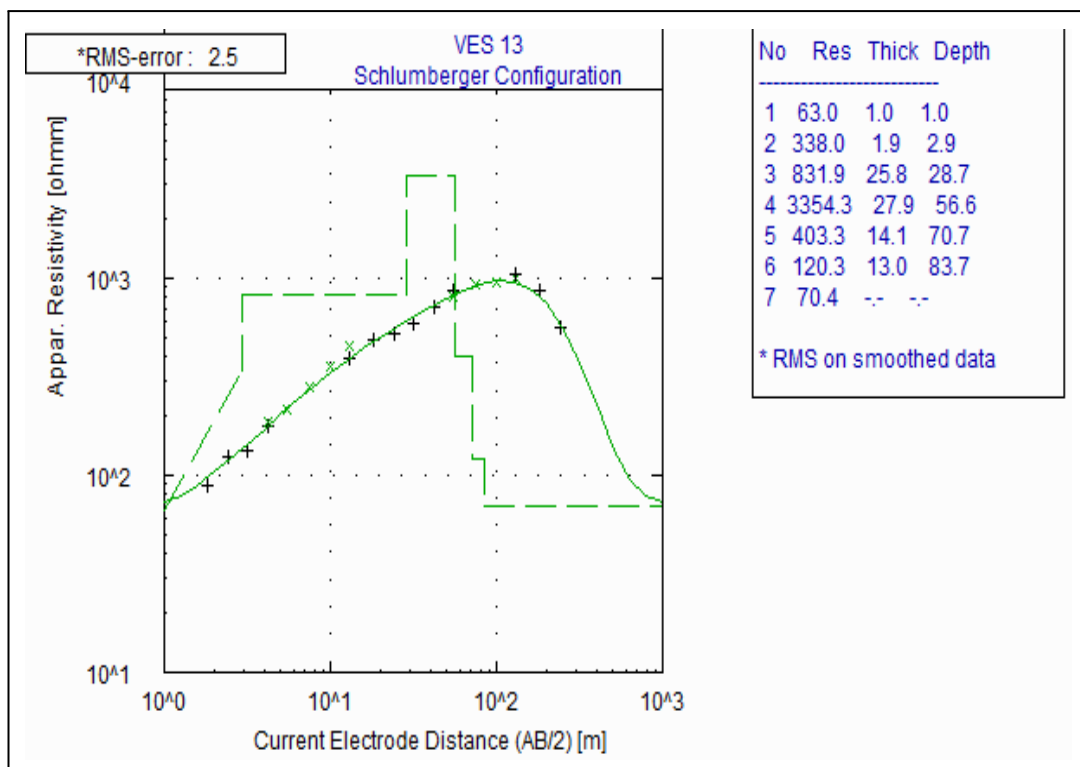


Figure 11. VES 13

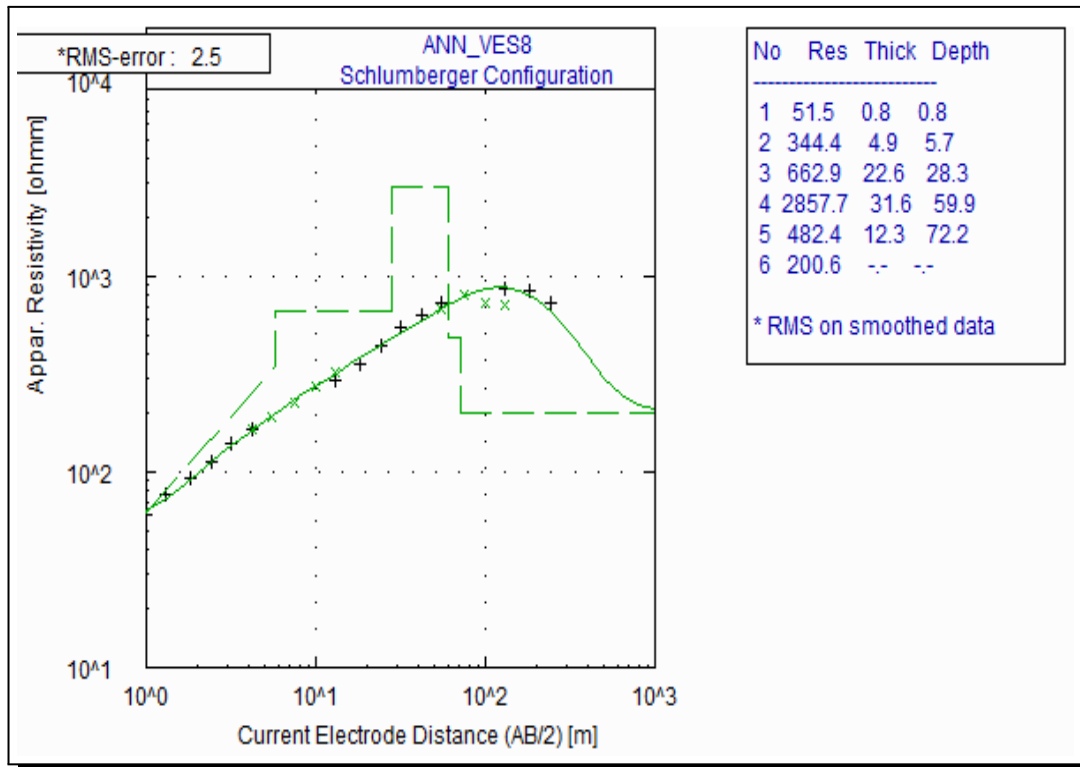


Figure 12. ANN_VES 8

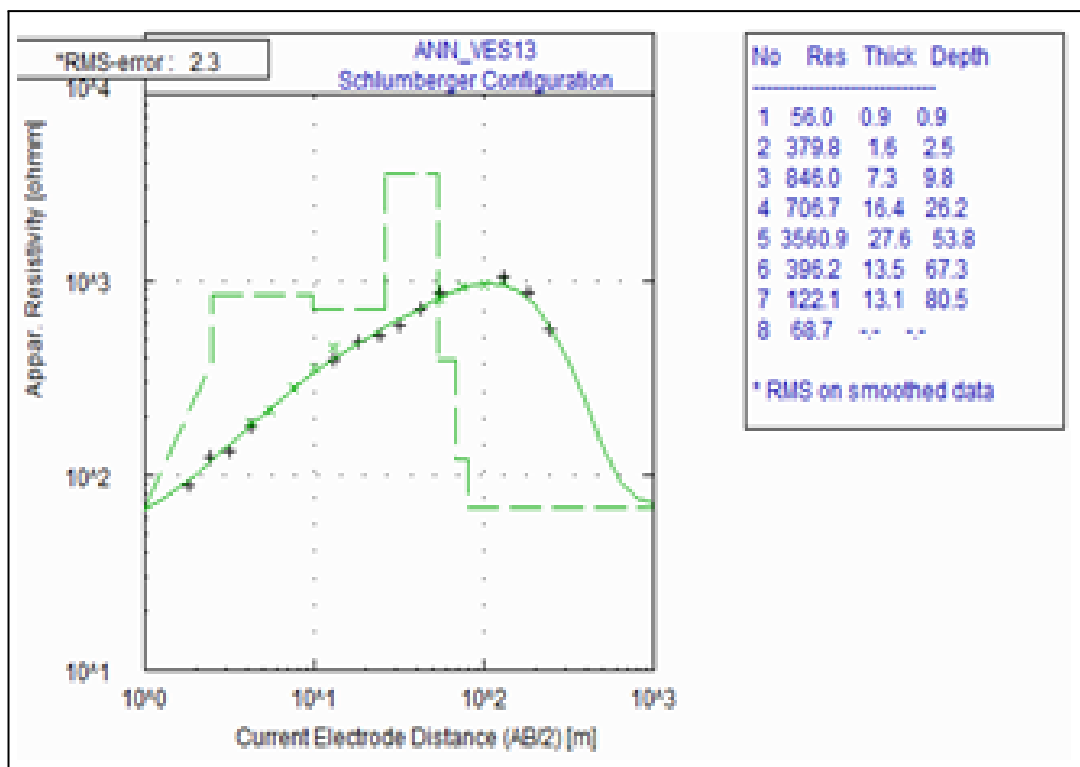


Figure 13. ANN_VES 13

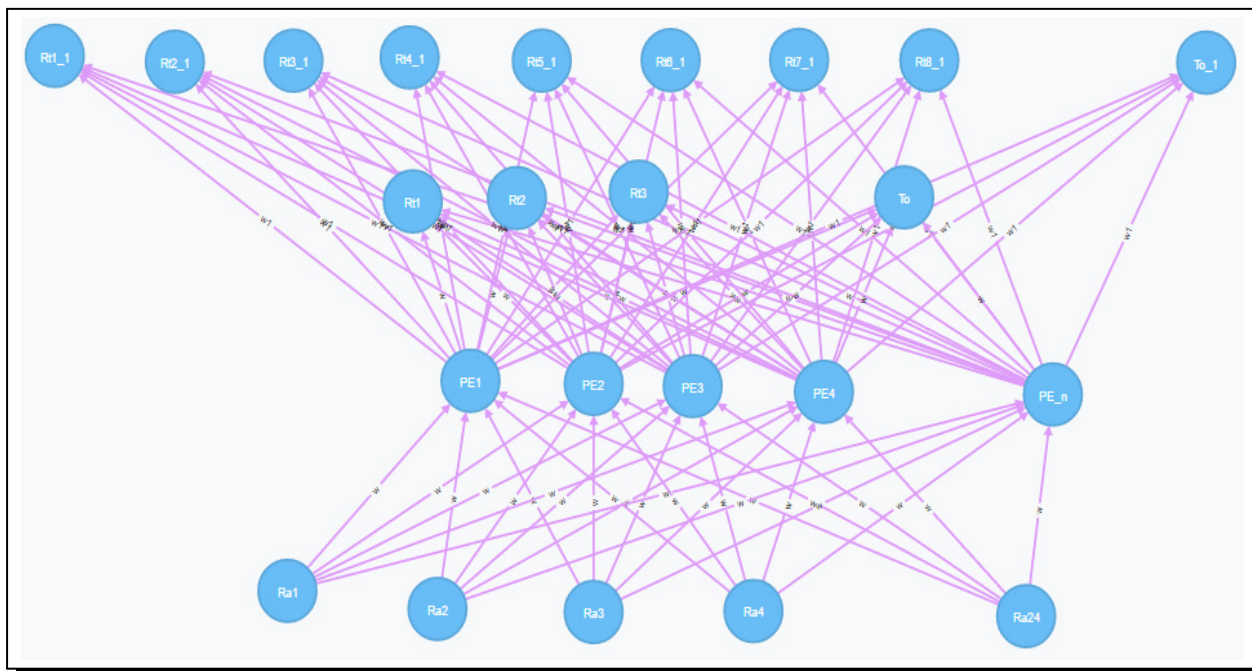


Figure 14. Neural network architecture

Acknowledgement

The authors appreciate Covenant University for partial sponsorship.

Competing Interests

The authors declare that they have no competing interests.

Authors' Contributions

All the authors contributed significantly in writing this article. The authors read and approved the final manuscript.

References

- [1] A.P. Aizebeokhai, 2D and 3D geoelectrical resistivity imaging: theory and field design, *Scientific Research and Essays* **5** (23), 3592 – 2605.
- [2] H. Demuth, M. Beale and M. Hagan, *Neural Network Toolbox*, 1st edition, Natick, Mass, MathWorks **9** (4), 259 – 265.
- [3] O. Koefoed, Resistivity sounding on an earth model containing transition layers with linear change of resistivity with depth, *Geophysical Prospecting* **27** (4), 862 – 868.
- [4] L. Lines and S. Treitel, A review of least-squares inversion and its application to geophysical problems, *Geophysical Prospecting* **32** (2), 159 – 186.
- [5] G.F. Luger and W.A. Stubblefield. *Artificial Intelligence: Structures and Strategies for Complex Problem Solving*, 2nd edition, Benjamin/Cumming Publishing, Redwood City, California, p. 850 (1993).

- [6] J.L. McClelland, D.E. Rumelhart and G.E. Hinton, *The Appeal of Parallel Distributed Processing, in Parallel Distributed Processing: Explorations in the Microstructure of Cognition Foundations*, MIT Press, Cambridge, p. 34 (1986).
- [7] J. Stephen, C. Manoj and S. Singh, A direct inversion scheme for deep resistivity sounding data using artificial neural networks, *Journal of Earth System Science* **113** (1) (2004), 49 – 66.
- [8] A. Tarantola, *Inverse Problem Theory and Methods for Model Parameter Estimation*, 1st edition, Society for Industrial and Applied Mathematics, Philadelphia, PA, p. 358 (2005).